Organic Electronics 14 (2013) 1570–1576

Contents lists available at SciVerse ScienceDirect

Organic Electronics

journal homepage: www.elsevier.com/locate/orgel

Doping of TIPS-pentacene via Focused Ion Beam (FIB) exposure

Rebecca Saive [a,b,c,*], Lars Mueller [a,c], Eric Mankel [a,d], Wolfgang Kowalsky [a,b], Michael Kroeger [a,b]

[a] InnovationLab GmbH, Speyerer Str. 4, 69115 Heidelberg, Germany
[b] TU Braunschweig, Institute for High-Frequency Technology, Schleinitzstr. 22, 38106 Braunschweig, Germany
[c] U Heidelberg, Kirchhoff-Institute for Physics, INF 227, 69120 Heidelberg, Germany
[d] TU Darmstadt, Institute of Material Science, Petersenstr. 32, 64287 Darmstadt, Germany

ARTICLE INFO

Article history:
Received 30 October 2012
Received in revised form 16 January 2013
Accepted 23 February 2013
Available online 4 April 2013

Keywords:
Doping
Focused Ion Beam (FIB)
Scanning Kelvin Probe Microscopy
XPS
TIPS-pentacene

ABSTRACT

We report on the influence of Focused Ion Beam (FIB) exposure on TIPS-pentacene layers which are often used in solution-processable organic field-effect transistors (OFETs) and in many cases yield a field-effect mobility in the order of 1 cm^2/V s. We exposed TIPS-pentacene layers to a Ga^+ ion beam and measured the device characteristics of OFETs. We observed a strong influence of the FIB on *J–V* characteristics of TIPS-pentacene-based devices and determined an increase in the OFET mobility and on–off ratio and a decrease of the threshold voltage. To further investigate the underlying process we analyzed FIB-exposed and unexposed TIPS-pentacene samples via X-ray Photoelectron Spectroscopy (XPS). Exposed samples show a clear Ga XPS signature and the C1s peak shifts about 400 meV towards smaller binding energies which is an indicator for a Fermi energy shift closer to the valence states and hence p-doping of TIPS-pentacene. With Scanning Kelvin Probe Microscopy (SKPM) we could clearly distinguish FIB exposed areas from the unexposed areas. For exposed areas the work function increases about 200 meV which is consistent with XPS measurements and again displays that the implanted Ga^+ ions serve as p-dopants. Furthermore we took SKPM measurements on operating OFETs and could investigate a dramatic change in local conductance on FIB exposed areas. This demonstrates a novel way of nanopatterning conductive paths in organic semiconductors.

1. Introduction

Tuning the charge transport properties of electronic materials is one of the most important challenges in semiconductor technology. Doping of semiconductors circumvents problems generally associated with low intrinsic conductivity and inefficient charge injection [1]. Yet, there has been reported on various doping techniques in inorganic as well as in organic materials to manipulate charge carrier concentration and mobility. A common technique for doping of organic semiconductors is coevaporation of the organic host material with either organic molecules or inorganic species [1,2]. For inorganic materials, ion implantation via Focused Ion Beam (FIB) has been demonstrated to be a useful doping technique and has been successfully applied to various semiconductor systems such as GaAs [3] and doping of Ge nanowires [4]. Here we apply ion implantation with a Ga^+ FIB to organic thin films. We use 6,13-bis(triisopropylsilylethynyl) pentacene (TIPS-pentacene) [5] to demonstrate ion implantation as it is widely employed for organic FETs. TIPS-pentacene or similar substituted pentacene derivatives regularly show mobilities in the range of 1 cm^2/V s or above and thus is an often used material system. Another major advantage is the processability from solution which makes them a promising candidate for printing applications [6]. Therefore controlled manipulation of the charge transport characteristics is strongly required. Recently a method to n-dope TIPS-pentacene from solution has been demonstrated [7]. Here we will present local p-doping of TIPS-pentacene

* Corresponding author at: InnovationLab GmbH, Speyerer Straße 4, 69115 Heidelberg, Germany. Tel.: +49 6221 5419 123.
E-mail address: rebecca.saive@innovationlab.de (R. Saive).

1566-1199/$ - see front matter © 2013 Elsevier B.V. All rights reserved.
http://dx.doi.org/10.1016/j.orgel.2013.02.040

which might play an auspicious role in micropatterned electronics.

2. Experimental

To investigate the properties of FIB-induced doping, we used TIPS-pentacene field effect transistors in a bottom gate, bottom contact device architecture. Heavily n-doped silicon wafers with 200 nm of thermally grown SiO_2 served as a substrate and constitute the gate contact and gate dielectric of our TFTs. The drain-source pattern was defined by photolithography and deposited by thermal evaporation of 10 nm aluminum (adhesive layer) and 60 nm gold. The channel length and width was 4 μm and 160 μm, respectively. Such small structures had to be chosen to allow for further treatment with the FIB which is designed for sample manipulation in the nanometer and micrometer range. For the experiments which are summarized in Figs. 1 and 3–5. TIPS-pentacene was drop-casted from solution in toluene onto the electrode structure as this preparation method has been demonstrated before to enable a good performance with a mobility up to 0.2 $cm^2/V\,s$ [8]. Note that we did not treat the substrates with a self assembled monolayer (SAM) like octadecyltrichlorosilane (OTS) or hexamethyldisilazane (HMDS) to have a as simple and controllable system as possible. Therefore we gained lower field effect mobilities of about $10^{-4}\ cm^2/V\,s$ which is consistent with the results of Anthony et al. [9]. For the conductance measurement in Fig. 2 the TIPS-pentacene was spin-coated to have better thickness and uniformity control. In these devices the layer thickness has been determined to be about 100 nm by FIB milling of the layer and afterwards SEM characterization of the milled edge.

Furthermore we used a Carl Zeiss AURIGA cross beam microscope to expose well defined areas in the OFET channels with the FIB. We operated the FIB at an acceleration voltage of 30 kV and adjusted the beam characteristics well outside the to be exposed sample area, to prevent from uncontrolled exposure before the actual experiment. To regulate the ion dose we varied the FIB current (emitted ions per time) and the exposure time.

To observe the influence of FIB on transistor characteristics one transistor was exposed several times and transistor characteristics were recorded in situ in the microscope after every exposure step. The field effect mobility has been derived from the slope of the OFET transfer curve at a source-drain voltage of 20 V. Threshold voltage and on–off-ratio have been extracted from the transfer curve as well.

The conductance measurements shown in Fig. 2 were performed on transistor structures without contacting the gate such that two terminal devices were created and the resistances were derived from the linear parts of the *IV* curves.

The photoemission spectra were taken in a PHI VersaProbe 5000 multitechnique analysis system equipped with a monochromated Al-Kα X-ray source and a hemispherical photoelectron analyzer. The energy scale of the spectrometers was calibrated to the Fermi energy position of a clean silver foil. Using a pass energy of 11 eV the energetic resolution of the system is about 350 meV at the Fermi edge.

We used a BRR-upgrade (from the company DME) of the Zeiss crossbeam workstation to perform atomic force microscopy (AFM) and scanning Kelvin probe microscopy (SKPM). In this combined system FIB exposure as well as SEM imaging and scanning probe microscopy (SPM) measurements can be performed simultaneously so that in-situ preparation and characterization without breaking the vacuum is possible. SKPM is a scanning probe technique which maps the contact potential difference (CPD) between the tip of the microscope and the sample surface [10]. The measured CPD is a superposition of the difference of the local surface work function [11] and the applied voltage. SKPM is a powerful tool to analyze charge transport as it has a spatial resolution down to 20 nm and an electrical resolution down to 10 mV [12].

3. Results and discussion

3.1. Doping of TIPS-pentacene transistors

We first observed the doping effect of FIB exposure when milling OFETs to study buried interfaces with SKPM.

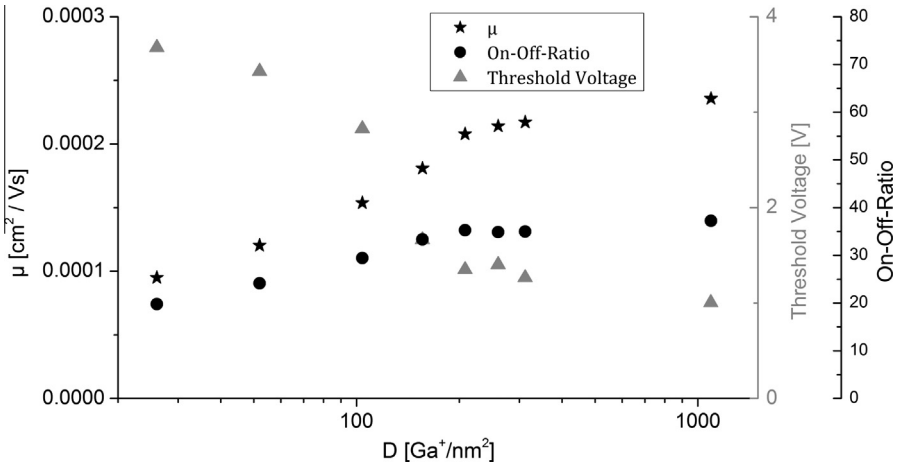

Fig. 1. Mobility, threshold voltage and on–off-ratio of a TIPS-pentacene OFET depending on the Ga^+ dose. The dose is given in Ga^+ ions per square nanometer.

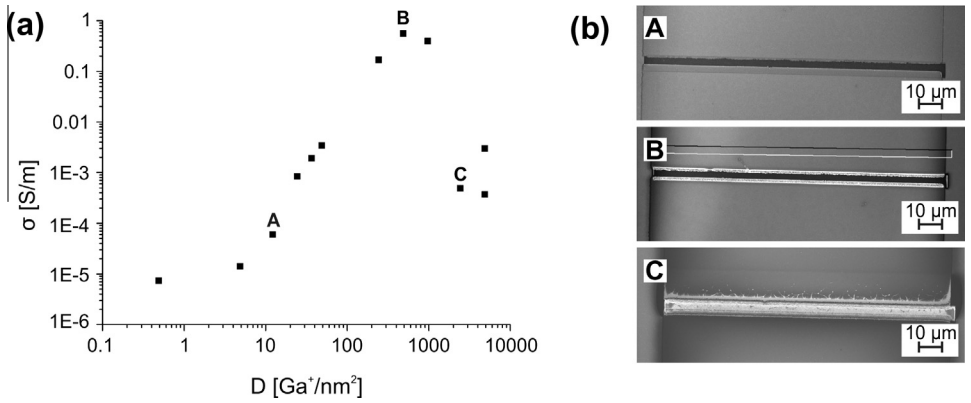

Fig. 2. (a) Conductivity of a two terminal device depending on the Ga^+ dose. (b) SEM images of the TIPS-pentacene covered source and drain contacts at different doses. The respective dose is marked in the diagram at the left. In **A** the FIB treated TIPS-pentacene appears darker than the untreated, **B** it appears even darker. In **C** one can see that the TIPS-pentacene layer was destroyed be the FIB.

Therefore we performed a controlled experiment of applying distinct doses of Ga^+ onto the active channel material. All output characteristics were indicating functioning TFT devices. Fig. 1 shows the field effect mobility, threshold voltage and on–off-ratio of a TIPS-pentacene OFET depending on the Ga^+ dose. Undoped OFETs had a mobility of about $1 \times 10^{-4}\,cm^2/V\,s$ which increased with the Ga^+ exposure up to $2 \times 10^{-4}\,cm^2/V\,s$. The threshold voltage drops from 4 V to 1 V and the on–off ratio slightly increases. A similar behavior could be observed in pentacene OFETs doped with MoO_3 as reported by Wang et al. [13]. For ordered semiconductors like crystalline silicon it was found that the mobility decreases with increasing doping concentration due to charge carrier scattering on defect states [14]. This situation gets less predictable for disordered systems. For example in amorphous silicon Street et al. found out that only the mobility of the minority charge carriers is affected upon doping [15]. In the case of this work organic field effect transistors with highly disordered morphology have been studied and the observed field effect mobility increase can be explained by two main effects: A reduction of the contact barrier between the source and drain contacts and the TIPS-pentacene and a filling of trap states in the organic and on the gate dielectric interface. The increase of mobility by filling of trap states has already been proposed by several groups [16,17] and has been observed for different materials [18] and doping systems [19]. Recently Olthof et al. have shown that with controlled ultralow doping a controlled mobility increase in C_{60} can be observed [20]. Their experimental results are in good agreement with kinetic Monte Carlo simulations and give an evidence for trap state filling.

As mentioned above the deduced field effect mobility can also be affected by change in the charge injection barrier from the electrodes to the channel material [1]. As the equations used to deduce the charge carrier mobility from the TFT transfer characteristic assume perfect carrier injection, any imperfection in carrier injection (e.g. injection barrier) will lead to a lower FET mobility, which might also be true for our samples. Now doping of the channel material can lower the injection barrier and hence will be reflected in a higher FET mobility for the doped sample. One might argue that FIB exposure will lead to a thinning of the channel layer and therefore may influence the OFET characteristics. But, in OFETs, charge accumulation is restricted to the interface between gate dielectric and semiconductor and only a few nanometers thin channel, which in our case is buried, will contribute to carrier transport [21]. Therefore it is unlikely that geometry changes in the channel area due to FIB induced material ablation lead to an observable change in the OFET characteristics.

The above presented results clearly show an effect of Ga^+ doping on OFETs and shall be further studied by conductivity measurements as in a doped system an increase of the conductivity must be expected [22].

In Fig. 2 the effect of FIB exposure on the conductance of a two terminal TIPS-pentacene device is shown. Fig. 2a presents the conductivity σ of the TIPS-pentacene in dependence of the dose D of Ga^+ ions. Three characteristic samples are marked with A, B, and C and help to identify three different regimes of how the applied dose correlates with the sample's conductivity. One observes a strong increase of nearly five orders of magnitude in conductivity with accumulated Ga^+ dose. Between samples A and B this increase follows a power law dependence $\sigma \propto D^n$ (with $n \approx 3$). Between B and C the conductance decreases abruptly and for doses higher than C one cannot find a clear relation. For comparison, Fig. 2b shows SEM images of the marked samples A, B and C. The source and drain contacts are covered with homogeneous layers of TIPS-pentacene and the subsequently exposed channels are displayed. In A the FIB exposed TIPS-pentacene in the channel appears darker than in the rest of the image and this difference in contrast becomes even stronger with additional Ga^+ doping as seen for sample B. In C one can see that the channel has been destroyed by the FIB which explains the drop of the conductivity in the second and third regime. The super proportional increase of the conductivity in the first regime can be explained on the one hand by generation of free charge carriers in the bulk and on the other hand by the mobility increase shown in Fig. 1. Additionally, remote doping of molecules deeper in the film, as

reported by Zhao et al. [22], may even lead to an increase in local conductivity below the penetration depth. The lowering of the OFET threshold voltage seen in Fig. 1 may be an indicator for this.

The conductance measurements were also performed on bare substrates without TIPS-pentacene layer to investigate whether the increase could also occur from substrate doping or forming of a Gallium metal film. The FIB had no influence on the conductivity of these structures for which reason we can be sure that the observed conductance changes are due to doping of the TIPS-pentacene.

Deriving an average mobility of 10^{-4} cm^2/V s from the data displayed in Fig. 1, the charge carrier density thus can be varied between 10^{17} cm^{-3} for undoped TIPS-pentacene (regime before A) and 10^{21} cm^{-3} for TIPS-pentacene doped to saturation (regime around B). The samples had been handled in air before they were inserted into the microscope. The high charge carrier density of 10^{17} cm^{-3} for the undoped TIPS-pentacene thus can be explained by impurity doping, e.g. oxygen from ambient air. Such a contamination can also explain why small Ga^+ doses (regime before A) do not have any influence on the conductivity and why a relatively small on–off-ratio was measured on the transistors. Note that, experimental uncertainties as contact resistance in the two terminal device and slight geometry variations (layer thickness, channel width and length) may lead to small errors in the absolute values. But unaffected, the results show, that controlled doping via Ga^+ ion implantation is also possible in organic materials.

3.2. XPS measurements

By XPS we studied the electronic changes upon Ga^+ ion beam doping. Therefore we exposed a 2 mm × 2 mm square on a TIPS-pentacene layer with FIB and took XPS spectra of an unexposed and the exposed area. Fig. 3 shows the corresponding XPS spectra for energies around the characteristic emission lines of Fig. 3a Ga2p, Fig. 3b Si2p, Fig. 3c C1s and Fig 3d O1s.

In Fig. 3a it is apparent that there is no Ga in the unexposed area but the exposed area shows a clear Ga2p signal which consists of a main peak at 1117.5 eV and a minor

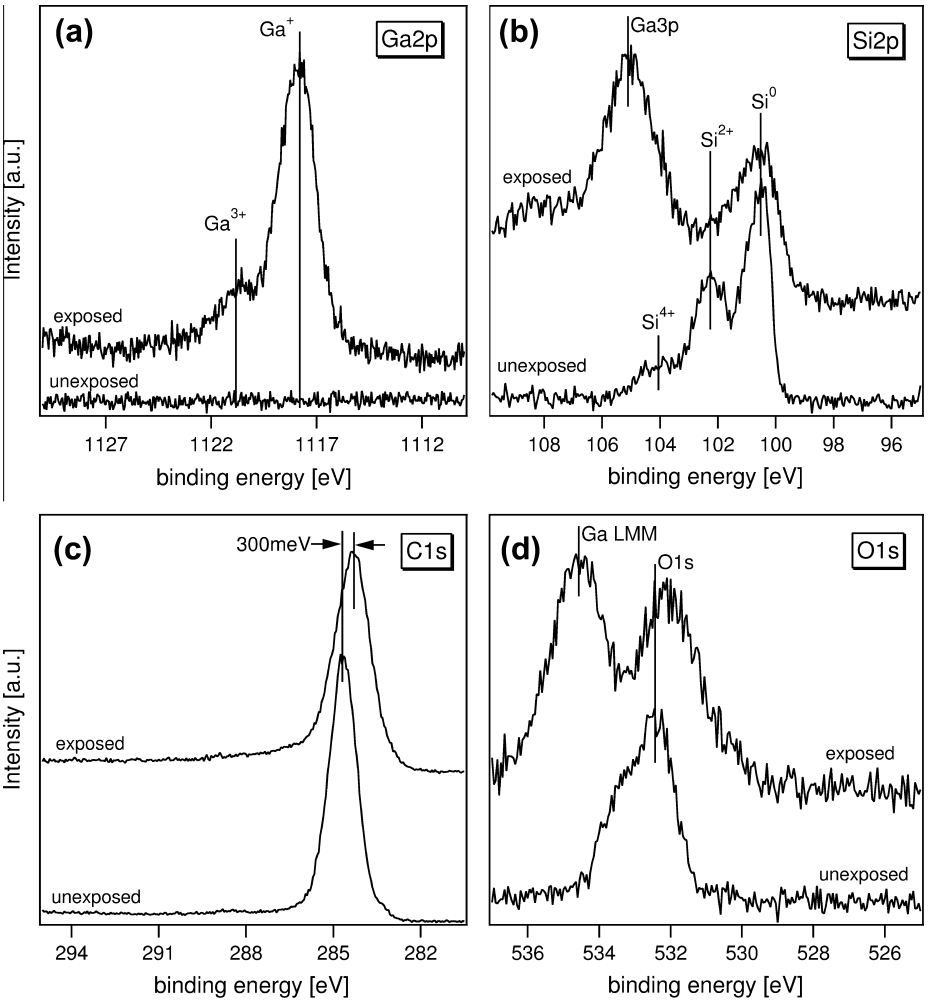

Fig. 3. XPS measurements on TIPS-pentacene before and after FIB exposure in the area of characteristic peaks: (a) Ga2p, (b) Si2p, (c) C1s, and (d) O1s.

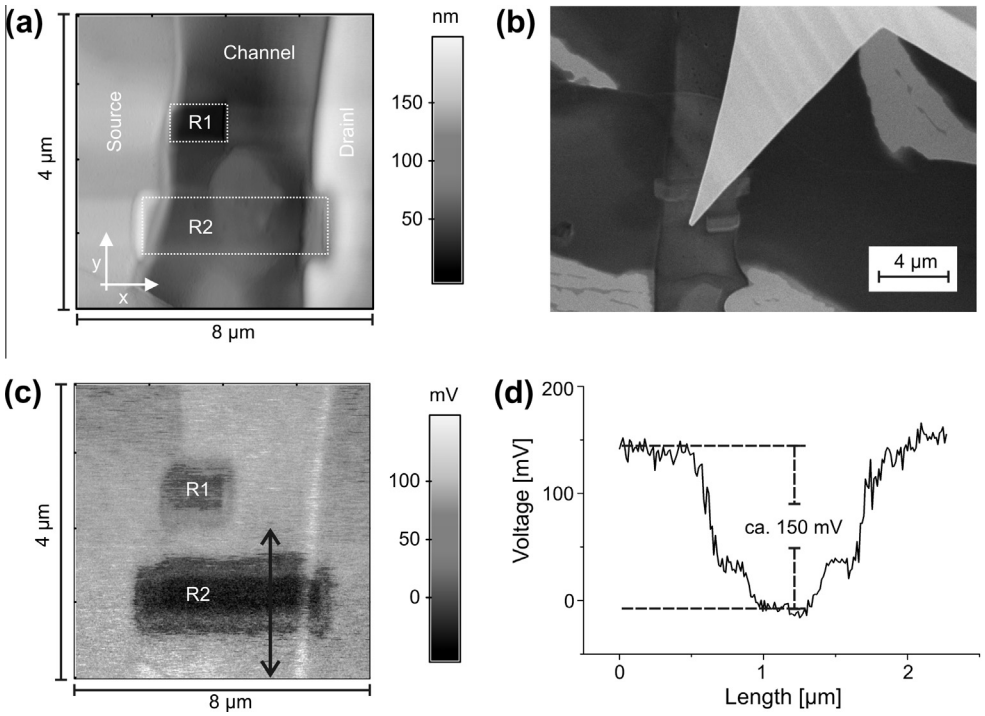

Fig. 4. (a) Topography image of a TIPS-pentacene OFET channel with two FIB exposed rectangular areas. The lower rectangle (R2) stretches laterally from source to drain contact thereby covering the whole channel in the *x*-direction. The upper one (R1) has only incomplete coverage of the channel and extends in *x*-direction from the source contact to about the center of the channel. (b) SEM image of the same area while in contact with an AFM cantilever. (c) SKPM measurement correlating to the topography shown above. The FIB treated rectangles are clearly distinguishable by the lower potential difference. (d) Profile of the SKPM signal marked by the arrow in (c).

peak at 1121 eV. The main peak can be attributed to Ga^+ ions, the minor peak is caused by Ga^{3+} ions. There is no metallic Ga present. Its emission line is found to peak at 1116.5 eV binding energy and should show the typical asymmetric line shape of a metal [23].

As a TIPS-pentacene molecule contains two Si atoms one can find a Si signature (Fig. 3b) in the unexposed TIPS-pentacene layer. The line shape shows three different components which can be attributed to three different oxidation states. The Si^0 component at 100.5 eV binding energy belongs to the TIPS-pentacene Si. As the difference of electronegativities between Si and C is only 0.6 (pauling scale) [24] the expected chemical shift of Si in TIPS-pentacene compared with pristine unoxidized Si is close to zero. A part of the TIPS-pentacene molecules at the surface seems to be oxidized resulting in the Si^{2+} component at 102.5 eV binding energy. The gate electrode of the transistor consists of SiO_2 and is not completely wetted by the TIPS-pentacene. This leads to the Si^{4+} shoulder at 104.5 eV binding energy. In the exposed case the silicon signal at 100.5 eV is still visible but most of the emission line at higher binding energies is overlapped by the strong signal of the Ga3p emission line.

The TIPS-pentacene layers were handled in air before the measurements therefore an oxygen signature was expected in both cases. Fig. 3d) confirms that the unexposed film contains oxygen. The O1s emission of the unexposed film shows two components whose origin is either the oxidized TIPS-pentacene at the surface or oxygen containing adsorbates (e.g. water or hydrocarbons) at the surface. After exposure the O1s signal is overlapped by a part of the Ga LMM auger emission line. However a part of the remaining oxygen seems to oxidize the Ga^+ ions forming Ga_2O_3 which is the stable gallium oxide phase. The Ga^{3+} ions of the oxide are visible in Fig. 3a).

The C1s corelevel is shown in Fig. 3c. The emission line of the unexposed sample has a symmetric shape according with the similar electronegativities of the TIPS-pentacene atoms (C, Si, H). The peak maximum is at 284.8 eV binding energy. For the exposed sample the maximum of the C1s line shifts about 400 meV to lower binding energies. Simultaneously the line width becomes slightly broader but does not show any additional chemically shifted component.

From the spectra it can be concluded that there is no serious chemical interaction (like oxidation) between the Ga ions and the TIPS-pentacene. The shift of the C1s core level line to smaller binding energies can be interpreted as Fermi level shift. In this case the Fermi energy of TIPS-pentacene shifts 400 meV closer to its valence states after Ga^+ exposure which is equivalent to p-doping of the material [25]. The doping can be explained by Ga^+ ions catching an electron from TIPS-pentacene after penetrating. Usually in opposite to the chemical shift indicating oxidation or reduction of atoms the Fermi level shift is much more sensitive to charge transfer. That is why no reduced Ga^0 component is obviously visible in the Ga2p spectra. The larger

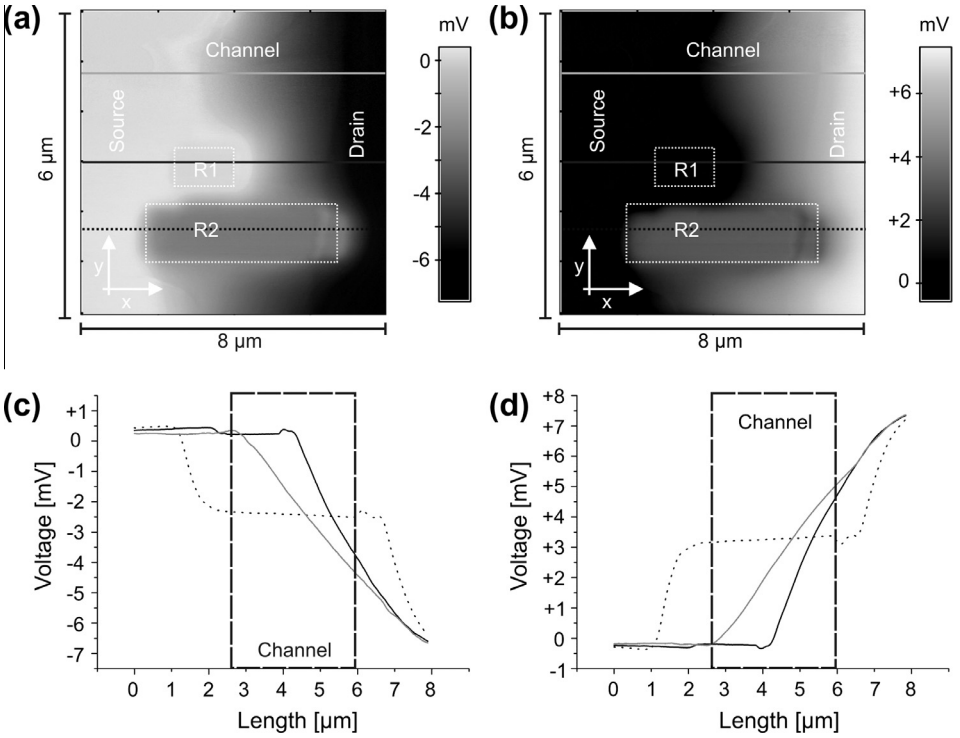

Fig. 5. SKPM measurement of the same TIPS-pentacene OFET channel as in Fig. 4 at (a) 10 V and (b) −10 V source-drain bias voltage and a gate voltage of 0 V. (c) Potential profiles at different positions in (a). The gray line corresponds to a non-exposed region, the black line marks a profile through R1 and the dotted curve belongs to a profile through R2. (d) Shows the corresponding profiles marked in (b).

width of the C1s emission line after exposure can be explained by a higher energetic disorder in the TIPS-pentacene film induced by the Ga^+ ions.

3.3. SKPM measurements

Fig. 4 shows different images of a TIPS-pentacene channel where two rectangular areas were exposed to the FIB. The lower rectangle (R2) stretches laterally from source to drain contact thereby covering the whole channel in the *x*-direction. The upper one (R1) has only incomplete coverage of the channel and extends in *x*-direction from the source contact to about the center of the channel. In Fig. 4a an AFM image of the area of interest is illustrated, where the FIB exposed area can be distinguished by lower height because of material ablation due to FIB sputtering. Fig. 4b shows a SEM image of the corresponding area during AFM characterization. The exposed rectangles are clearly visible by the brighter appearance compared to the rest of the film. In Fig. 4c the SKPM measurement at 0 V source-drain voltage is presented. The FIB exposed areas can be identified by the lower SKPM signal. The SKPM signal is always a superposition of the work function difference between tip and sample and the applied voltage or charging. A local charging can be excluded as the material conducts quite well and the SKPM images did not change with time. Furthermore there was no voltage applied to the contacts, a local variation of the electric field therefore can be excluded and the measured signal difference must result from the work function difference. A lower SKPM signal of the exposed area means that the work function in this area is higher. A higher work function can be caused by a shift of the Fermi energy towards the HOMO which is an evidence for p-doping of the TIPS-pentacene. Fig. 4d shows a profile through an exposed and a non-exposed area and one can find a work function difference of about 150 mV.

In Fig. 5 SKPM measurements of the same sample as in Fig. 4 but while applying a source-drain voltage of 10 V (Fig. 5a) and −10 V (Fig. 5b) is shown. Fig. 5c and d shows profiles of the respective SKPM measurement along the channel for three different positions. The gray line corresponds to a non-exposed area, the black line marks a profile through R1 and the dotted line belongs to a profile through R2. For the unexposed area the surface potential is constant in the contact areas and drops within the channel. At the drain contact the potential does not stay constant. This is due to an interaction between the whole cantilever and the sample surface and is a known measurement artefact in SKPM measurements [26]. In R1, the potential is on a constant level throughout the drain contact and the exposed channel area, but drops over the non-exposed channel area. The potential in R2 sharply drops at the contact-channel-boundaries, but stays constant through the (exposed) channel area and throughout the contact area. Qualitatively, the devolution for 10 V vs. −10 V applied bias is the same. The gray line (non-exposed channel) represents an often-measured potential

distribution of an OFET channel, where grain boundary effects are insignificant. The potential drops along the channel as this is the part with the highest resistance. The black line (partially exposed channel) can be explained equivalently: The doping lowers the resistance of the TIPS-pentacene and the potential drops along the undoped part of the channel. To understand the shape of the dotted curve (exposed channel) one has to remind the device architecture. The TIPS-pentacene film sits on top of the contact and the doping molecules are inserted from the top. That means that the upper part of the TIPS-pentacene layer has a lower resistance than the subjacent part. As a consequence the current flows from the source contact in nearly vertical direction to the upper part, passes the channel via the upper part and flows vertically down to the drain contact. The highest resistance which has to be overcome is then the vertical path from contact to upper layer and vice versa. This explains the sharp surface potential drops at the boundary between the electrode and channel areas.

These results demonstrate that local doping via a Ga^+ FIB with high resolution is possible and can be used to nanopattern conductive pathways for organic devices.

4. Summary

We studied the effect of FIB exposure on TIPS-pentacene. We could observe a strong increase of the conductivity with increasing ion dose. In a TIPS-pentacene FET the mobility and the on–off ratio increased and the threshold voltage decreased. By XPS and SKPM characterization, we demonstrated that p-doping is evident. SKPM analyses on a biased OFET sample have shown that the conductivity manipulation can be performed with high lateral resolution. A potential application of the demonstrated technique can be local p-doping to control charge injection or conductance in organic nanoscale devices.

Acknowledgements

We acknowledge the German Federal Ministry of Education and Research (BMBF) for generous financial support (FKZ 13N10794 and FKZ 13N10723).

References

[1] K. Walzer, B. Maennig, M. Pfeiffer, K. Leo, Highly efficient organic devices based on electrically doped transport layers, Chemical Reviews 107 (2007) 1233–1271.
[2] M. Kroeger, S. Hamwi, J. Meyer, T. Riedl, W. Kowalsky, A. Kahn, P-type doping of organic wide band gap materials by transition metal oxides: a case-study on molybdenum trioxide, Organic Electronics 10 (2009) 932–938.
[3] Y. Hirayama, H. Okamoto, Electrical properties of ga ion beam implanted gaAs epilayer, Japanese Journal of Applied Physics 24 (1985) L965–L967.
[4] T. Burchhart, C. Zeiner, A. Lugstein, C. Henkel, E. Bertagnolli, Tuning the electrical performance of ge nanowire MOSFETs by focused ion beam implantation, Nanotechnology 22 (2011) 035201.
[5] J.E. Anthony, D.L. Eaton, S.R. Parkin, A road map to stable, soluble, easily crystallized pentacene derivatives, Organic Letters 4 (2002) 15–18.
[6] S.H. Lee, M.H. Choi, S.H. Han, D.J. Choo, J. Jang, S.K. Kwon, High-performance thin-film transistor with 6,13-bis(triisopropylsilylethynyl) pentacene by inkjet printing, Organic Electronics 9 (2008) 721–726.
[7] Y. Qi, S.K. Mohapatra, S.B. Kim, S. Barlow, S.R. Marder, A. Kahn, Solution doping of organic semiconductors using air-stable n-dopants, Applied Physics Letters 100 (2012) 083305.
[8] C.S. Kim, S. Lee, E.D. Gomez, J.E. Anthony, Y.-L. Loo, Solvent-dependent electrical characteristics and stability of organic thin-film transistors with drop cast bis(triisopropylsilylethynyl) pentacene, Applied Physics Letters 93 (2008). 103302–103302-3.
[9] C. Sheraw, T. Jackson, D. Eaton, J. Anthony, Functionalized pentacene active layer organic thin-film transistors, Advanced Materials 15 (2003) 2009–2011.
[10] M. Nonnenmacher, M.P. O'Boyle, H.K. Wickramasinghe, Kelvin probe force microscopy, Applied Physics Letters 58 (1991) 2921–2923.
[11] D. Cahen, A. Kahn, Electron energetics at surfaces and interfaces: concepts and experiments, Advanced Materials 15 (2003) 271–277.
[12] W. Melitz, J. Shen, A.C. Kummel, S. Lee, Kelvin probe force microscopy and its application, Surface Science Reports 66 (2011) 1–27.
[13] Z. Wang, M. Waqas Alam, Y. Lou, S. Naka, H. Okada, Enhanced carrier injection in pentacene thin-film transistors by inserting a moO3-doped pentacene layer, Applied Physics Letters 100 (2012). 043302–043302-4.
[14] D. Caughey, R. Thomas, Carrier mobilities in silicon empirically related to doping and field, Proceedings of the IEEE 55 (1967) 2192–2193.
[15] R.A. Street, J. Zesch, M.J. Thompson, Effects of doping on transport and deep trapping in hydrogenated amorphous silicon, Applied Physics Letters 43 (1983) 672–674.
[16] Y. Qi, T. Sajoto, S. Barlow, E.-G. Kim, J.-L.B., S.R. Marder, A. Kahn, Use of a high electron-affinity molybdenum dithiolene complex to p-dope hole-transport layers, Journal of the American Chemical Society 131 (2009) 12530–12531 (PMID: 19678703).
[17] Y. Zhang, B. de Boer, P.W.M. Blom, Trap-free electron transport in poly(p-phenylene vinylene) by deactivation of traps with n-type doping, Physical Review B 81 (2010) 085201.
[18] X. Jiang, Y. Harima, K. Yamashita, Y. Tada, J. Ohshita, A. Kunai, Doping-induced change of carrier mobilities in poly(3-hexylthiophene) films with different stacking structures, Chemical Physics Letters 364 (2002) 616–620.
[19] B. Maennig, M. Pfeiffer, A. Nollau, X. Zhou, K. Leo, P. Simon, Controlled p-type doping of polycrystalline and amorphous organic layers: self-consistent description of conductivity and field-effect mobility by a microscopic percolation model, Physical Review B 64 (2001) 195208.
[20] S. Olthof, S. Mehraeen, S.K. Mohapatra, S. Barlow, V. Coropceanu, J.-L. Brédas, S.R. Marder, A. Kahn, Ultralow doping in organic semiconductors: evidence of trap filling, Physical Review Letters 109 (2012) 176601.
[21] F. Dinelli, M. Murgia, P. Levy, M. Cavallini, F. Biscarini, D.M. de Leeuw, Spatially correlated charge transport in organic thin film transistors, Physical Review Letters 92 (2004) 116802.
[22] W. Zhao, Y. Qi, T. Sajoto, S. Barlow, S.R. Marder, A. Kahn, Remote doping of a pentacene transistor: control of charge transfer by molecular-level engineering, Applied Physics Letters 97 (2010) 123305.
[23] J.F. Moulder, W.F. Stickle, P.E. Sobol, K.D. Bomben, Handbook of X-ray Photoelectron Spectroscopy, ULVAC-PHI, Inc., 1995.
[24] C.E. Mortimer, U. Mueller, Chemie, 2007.
[25] T. Mayer, C. Hein, E. Mankel, W. Jaegermann, M.M. Mueller, H.-J. Kleebe, Fermi level positioning in organic semiconductor phase mixed composites: the internal interface charge transfer doping model, Organic Electronics 13 (2012) 1356–1364.
[26] D.S.H. Charrier, M. Kemerink, B.E. Smalbrugge, T. de Vries, R.A.J. Janssen, Real versus measured surface potentials in scanning kelvin probe microscopy, ACS Nano 2 (2008) 622–626.